

An Analytical Idealization of Longitudinal Bar Pull-out Effect for Seismic Response Analysis of Bridges



T. Sasaki

National Research Institute for Earth Science and Disaster Prevention

K. Kawashima

Tokyo Institute of Technology

K. Kajiwara

National Research Institute for Earth Science and Disaster Prevention

SUMMARY:

Column rotation occurs at the base if longitudinal bars yield and pull out from footing and column, and this contributes to develop additional lateral displacement of the deck. This paper describes development of a new column and footing interface element model which can realistically represent pull out of longitudinal bar effect taking the displacement integrity between a column and a footing, and shows evaluation of pull out of longitudinal bar effect and verification of the developed model based on the C1-5 column shake table experiment, which is the E-Defense full-scale shake table experiment on a typical RC column designed based on the 2002 code (C1-5 column). It is found from the result of seismic response analysis for C1-5 column that implementation of the proposed analytical model enhances the analytical correlation of the shake table experiment of the RC column designed in accordance with the current code.

Keywords: seismic design, bridge, RC column, pulling out of longitudinal bars, nonlinear dynamic analysis

1. INTRODUCTION

A column rotates not only by flexure but also rotation induced by longitudinal bar yielding and pulling out from inside footing and the column. This additionally contributes to develop a lateral displacement of the deck and affects the dynamic response of a bridge as shown in Fig. 1. This is defined hereinafter as pulling-out of longitudinal bars from a footing (PLB/F) and a column (PLB/C). The PLB/F and PLB/C effects are often disregarded or indirectly considered in analysis by artificially increasing column length at the base. For example, Priestley proposed to consider the effect by defining column base below the actual column base (Priestley 1996). However the PLB effect affects the seismic response of bridges, it is necessary to develop more rigorous model.

The column rotation due to yielding and pulling out of longitudinal bars was first recognized by Poprov (1984). He conducted loading experiments of RC beam-column joints and clarified that the effect of rotation at the joint was significant.

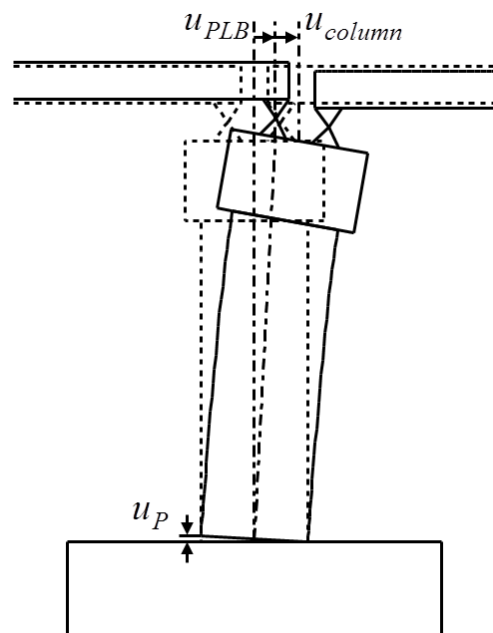


Figure 1. Column Rotation at the Column Base due to Pulling out of Longitudinal Bars

Several analytical models were developed for evaluation of bond stress-slip displacement hysteresis. For example, Shima et al. (1987) conducted pullout experiments of a 19 mm diameter deformed bar

bonded in a 500 mm diameter concrete cylinder and the developed an empirical model for evaluation of bond stress-slip displacement hysteresis. Imai et al. (2005) developed an analytical model for column rotation based on bond stress-slip displacement hysteresis model by Shima et al. (1987) and Morita (1969) resulting from cyclic loading for steel bolts bonded in a footing.

In this paper, an analytical model for PLB effect is proposed and its application to shown to a full scale RC bridge column.

2. DEVELOPMENT OF AN ANALYTICAL MODEL FOR PLB EFFECT

2.1. Interface Elements at Column Base

A column and footing interface element is defined as shown in Fig. 2 to represent the PLB effect considering the force equilibrium and displacement compatibility between a column base and its footing. The flexural moment at the base around two horizontal axes M_{Px} and M_{Py} and the vertical force F_{Pz} may be evaluated as

$$\begin{aligned} M_{Px}(\theta_x, \theta_y, u_z) &= \sum_{i=1}^N F_{PSi}(u_{Pi}) \times y_i + \sum_{i=1}^N F_{PCi}(u_{Pi}) \times y_i \\ M_{Py}(\theta_x, \theta_y, u_z) &= \sum_{i=1}^N -F_{PSi}(u_{Pi}) \times x_i + \sum_{i=1}^N -F_{PCi}(u_{Pi}) \times x_i \\ F_{Pz} &= \sum_{i=1}^N F_{PSi}(u_{Pi}) + \sum_{i=1}^N F_{PCi}(u_{Pi}) \end{aligned} \quad (1)$$

where θ_x and θ_y are rotation at the base about x and y horizontal axes, u_z is vertical displacement at the center of column section, x_i and y_i represent the location of the i -th longitudinal bar in x and y horizontal axes, u_{Pi} is a pullout displacement of the i -th longitudinal bar, F_{PSi} are pullout force of the i -th longitudinal bar and F_{PCi} is a resisting force due to concrete.

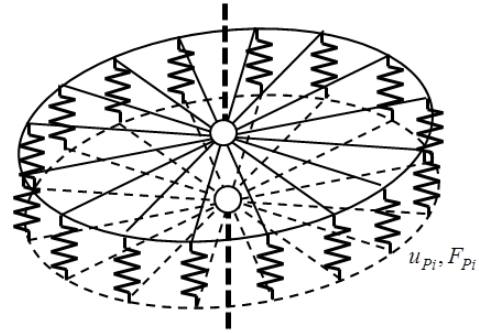


Figure 2. Column-Footing Interface Model for PLB

In this study, the section at the column base is assumed to remain the plain after deformation. Therefore, pull out displacement u_{Pi} can be evaluated from θ_x , θ_y and u_z as,

$$u_{Pi}(\theta_x, \theta_y, u_z) = \theta_x y_i - \theta_y x_i + u_z \quad (2)$$

2.2. Resisting Force of Longitudinal Bars

A pull out force vs. pull out displacement of a longitudinal bar is assumed as shown in Fig. 3, in which pullout displacement due to PLB in the i -th longitudinal bar, u_{Pi} , is assumed to be evaluated as

$$u_{Pi} = u_{PFi} + u_{PCi} \quad (3)$$

where u_{PCi} and u_{PFi} are pullout displacement due to PLB/C and PLB/F, respectively. A pull out displacement from a footing u_{PFi} may be evaluated based on the strain distribution of the bar in the footing, $\varepsilon(z)$, as

$$u_{PFi} = \int_{-H}^0 \varepsilon_F(z) dz \quad (4)$$

where H is the distance between the surface of the footing and the depth where strain of the bar becomes zero.

The bar strains inside the footing, $\varepsilon_F(z)$, are assumed as (refer to Fig. 4)

$$\varepsilon_F(z) = \begin{cases} \varepsilon_{Fe}(z) & (0 \leq \varepsilon_0 \leq \varepsilon_y) \\ \varepsilon_{Fe}(z) + \varepsilon_{Fp}(z) & (\varepsilon_0 > \varepsilon_y) \end{cases} \quad (5)$$

$$\varepsilon_{Fe}(z) = \begin{cases} \left(1 + \frac{z}{l_{PF}}\right) \varepsilon_0 \leq \left(1 + \frac{z}{l_{PF}}\right) \varepsilon_y & (-l_{PF} < z \leq 0) \\ 0 & (z \leq -l_{PF}) \end{cases} \quad (6)$$

$$\varepsilon_{Fp}(z) = \begin{cases} \left(1 + \frac{z}{\beta l_{PF}}\right) (\varepsilon_0 - \varepsilon_y) & (-\beta l_{PF} < z \leq 0) \\ 0 & (z \leq -\beta l_{PF}) \end{cases} \quad (7)$$

where z is a coordinate in the vertical axis ($z = 0$ at the top of the footing), $\varepsilon_{Fe}(z)$ and $\varepsilon_{Fp}(z)$ are the elastic and plastic strains inside footing, respectively, ε_0 is the strain of a longitudinal bar at the column base, ε_y is the yield strain of longitudinal bars, l_{PF} is the bond-degrading length inside the footing, which is the length of the region where the bond between the longitudinal bars and concrete deteriorated, and β is plastic strain development ratio, which is the ratio of the length of the region where longitudinal bars yield in the footing to the bond-degrading length, l_{PF} .

In this study, l_{PF} is assumed based on JSCE 2007 as,

$$l_{PF} = \frac{\sigma_y}{4\tau} \phi \quad (8)$$

$$\tau_a = 0.28\sigma_{ck}^{2/3} \quad (9)$$

where σ_y is the yield strength of the longitudinal bar and σ_{ck} is the concrete strength.

On the other hand, pullout displacement due to PLB/C, u_{PC} , is difficult to evaluate because two components of the strains of longitudinal bars in the column; 1) strains due to deformation of the column and 2) strains due to PLB/C, cannot be separated. Therefore, strain distribution due to PLB/C is assumed to be similar with the distribution defined by Eq. 5 as,

$$u_{PC} = \int_0^{l_{PC}} \varepsilon_C(z) dz \quad (10)$$

$$\varepsilon_C(z) = \begin{cases} \varepsilon_{Ce}(z) & (0 \leq \varepsilon_0 \leq \varepsilon_y) \\ \varepsilon_{Ce}(z) + \varepsilon_{Cp}(z) & (\varepsilon_0 > \varepsilon_y) \end{cases} \quad (11)$$

$$\varepsilon_{Ce}(z) = \left(1 + \frac{z}{l_{PC}}\right) \varepsilon_0 \leq \left(1 + \frac{z}{l_{PC}}\right) \varepsilon_y \quad (12)$$

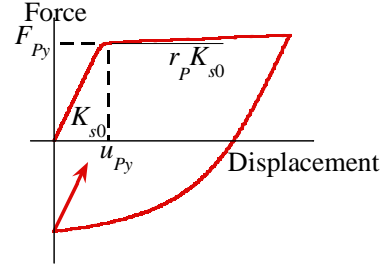


Figure 3. A Pull Out Force of Longitudinal Bar vs. Displacement Hysteresis for PLB

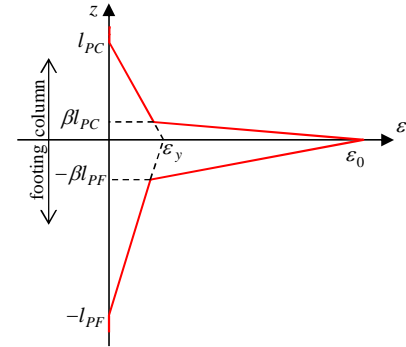


Figure 4. Assumed Strain Distribution in the Footing due to PLB

$$\varepsilon_{Cp}(z) = \begin{cases} \left(1 + \frac{z}{\beta l_{PC}}\right)(\varepsilon_0 - \varepsilon_y) & (0 \leq z < \beta l_{PC}) \\ 0 & (z \geq \beta l_{PC}) \end{cases} \quad (13)$$

where l_{PC} is the bond-degrading length inside the column. In this study, l_{PC} is assumed as

$$l_{PC} = \gamma l_{PF} \quad (14)$$

where γ is the bond-degrading ratio. It should be noted that when the distance between bottom of a longitudinal bar in the footing and the top of the footing, H , is deep enough ($H > l_{PF}$), the PLB/C displacement, u_{PC} , can be simply written as,

$$u_{PC} = \gamma u_{PF} \quad (15)$$

Based on Eqs. 1-12, the yield PLB displacement u_{Py} , the yield PLB force F_{Py} and the post yield stiffness ratio of PLB model r_p is derived as (refer to Fig. 3)

$$u_{Py} = \int_{-H}^0 \varepsilon_F(z) dz \Big|_{\varepsilon=\varepsilon_y} + \int_0^{l_{PC}} \varepsilon_C(z) dz \Big|_{\varepsilon=\varepsilon_y}$$

$$= \begin{cases} \frac{1}{2} \varepsilon_y (l_{PF} + l_{PC}) & (l_{PF} < H) \\ \frac{1}{2} \varepsilon_y \left\{ H \left(2 - \frac{H}{l_{PF}} \right) + l_{PC} \right\} & (l_{PF} \geq H) \end{cases} = \begin{cases} \frac{1+\gamma}{2} \varepsilon_y l_{PF} & (l_{PF} < H) \\ \frac{1}{2} \varepsilon_y l_{PF} \left\{ \frac{H}{l_{PF}} \left(2 - \frac{H}{l_{PF}} \right) + \gamma \right\} & (l_{PF} \geq H) \end{cases} \quad (16)$$

$$F_{Py} = \sigma_y A_l \quad (17)$$

$$r_p = \frac{F_P - F_{Py}}{u_P - u_{Py}} \Big/ \frac{F_{Py}}{u_{Py}} = \begin{cases} \frac{r_l}{\beta} & (l_{PF} < H) \\ \frac{r_l}{\beta(1+\gamma)} \left\{ \frac{H}{l_{PF}} \left(2 - \frac{H}{l_{PF}} \right) + \gamma \right\} & (l_{PF} \geq H) \end{cases} \quad (18)$$

where A_l is the cross section area of a longitudinal bar and r_l is the post yield stiffness ratio, which is the ratio of the post yield stiffness of longitudinal bars to young's modulus of longitudinal bars.

Resisting force of longitudinal bars should be related to the stress-strain relation of longitudinal bars. Therefore, the unloading and reloading rules for evaluation of force-displacement relation of PLB response of longitudinal bars is assumed to be same with the rules developed for the stress-strain relation of reinforcing bars by Menegotto-Pinto (1973) and modified by Sakai et al. (2003) in this study.

2.3. Resisting Force due to Concrete

Fig. 5 shows a resisting force due to concrete vs. pull out displacement hysteresis for idealizing the PLB. Because concrete generally spalled off and crashes at the column base and concrete in the footing does not crash, concrete in the footing can be assumed to be rigid in compression, while concrete does not resist in tension. Thus, F_{PCi} is assumed as,

$$F_{PCi}(u_{Pi}) = \begin{cases} K_{c0} u_{Pi} & (u_{Pi} < 0) \\ 0 & (u_{Pi} \geq 0) \end{cases} \quad (19)$$

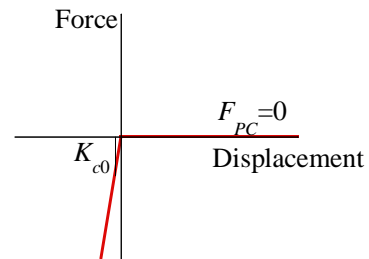


Figure 5. A Resisting Force due to Concrete vs. Displacement Hysteresis for PLB

$$K_{c0} = 1000 \frac{F_{Py}}{u_{Py}} \quad (20)$$

3. EVALUATION OF PLB IN THE FULL-SCALE RC BRIDGE COLUMN USED FOR THE E-DEFENSE SHAKE TABLE EXPERIMENT

Photo 1 shows the experimental setup of a full-scale RC column (C1-5) using E-Defense (Kawashima et al., 2009). C1-5 was a 7.5 m tall reinforced concrete column with a diameter of 2 m as shown in Fig. 6. C1-5 was designed in accordance with the 2002 JRA Design Specifications of Highway Bridges (JRA 2002). Sixty four deformed 35mm diameter longitudinal bars were provided in two layers. Deformed 22 mm diameter circular ties were set at 150 mm and 300 mm interval in the outer and inner longitudinal bars, respectively. The longitudinal



Photo 1. Setup of C1-5 experiment

reinforcement ratio P_l was 2.02 % and the volumetric tie reinforcement ratio ρ_s was 0.92 %. The longitudinal and tie bars had a nominal strength of 345 MPa (SD345), and the design concrete strength was 27 MPa. Based on the tensile tests, yield strength, tensile strength and Young's modulus of the longitudinal bars were 364 MPa, 562 MPa and 189 GPa, respectively.

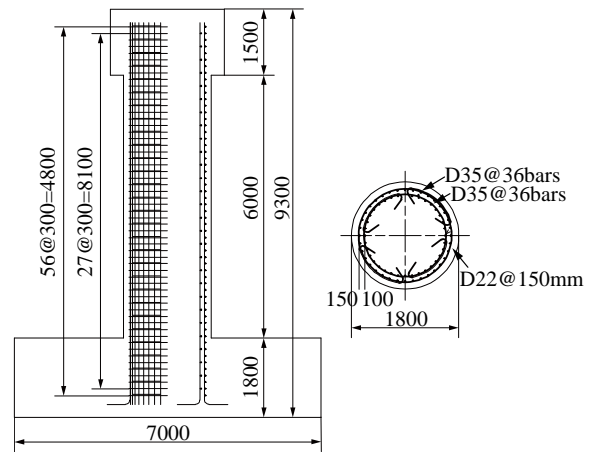


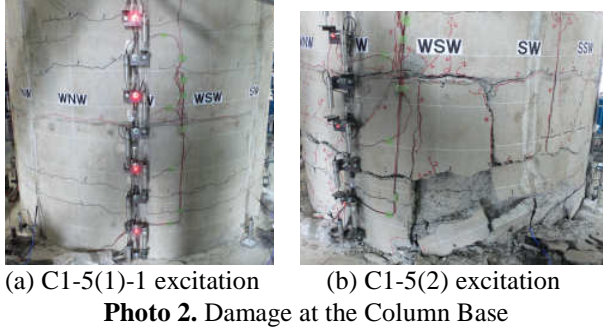
Figure 6. C1-5 Column

Two simply supported decks were set on the column and on the two steel end supports. Tributary mass to the column by two decks including four weights was 307 t and 215 t in the longitudinal and transverse directions, respectively.

C1-5 was excited using a near-field ground motion, which was recorded at the JR Takatori Station during the 1995 Kobe earthquake. It was one of the most influential ground motions to structures. However duration was short. Taking account of the soil structure interaction, a ground motion with 80% the original intensity of JR Takatori record was imposed as a command to the table in the experiment. This ground motion is called hereinafter as the 100 % E-Takatori ground motion. Excitation was repeated to clarify the seismic performance of the columns when they were subjected to near-field ground motions with longer duration and/or stronger intensity. C1-5 was excited five times. In the first twice, 100% E-Takatori ground motion was used (C1-5(1)-1 and C1-5(1)-2). After that, deck mass increased by 21 %, and C1-5 was excited once using 100% E-Takatori ground motion (C1-5(2)) and twice using 125 % E-Takatori ground motion (C1-5(3)-1 and C1-5(3)-2).

Photo 2 shows the damage at the column base after C1-5(1)-1 and C1-5(2) excitations. During C1-5(1)-1 excitation, only a few flexural cracks with the maximum width of 1mm occurred around the column at the plastic hinge. The damage progressed during C1-5(2) excitation such that the covering concrete spalled off at the 500 mm base zone from WSW to SSW.

Fig. 7 shows the response displacement at the column top in C1-5(1)-1 and C1-5(2) excitations in the principal response direction, which is the direction where the peak column displacement occurred. Lateral displacement due to PLB described later is also shown in Fig. 7. The peak displacements were 84 mm (1.1 % drift) and 254 mm (3.2 % drift) during C1-5(1)-1 and C1-5(2) excitations, respectively.



It is noted that the ultimate displacement in accordance with JRA 2002 code was 235 mm in C1-5 column, respectively.

Fig. 8 shows strain distributions of a NE longitudinal bar inside footing when the column displacement reached its peak during C1-5(1)-1 and C1-5(2) excitations. During C1-5(1)-1 excitation, outer and inner longitudinal bars at the top of the footing and 150 mm below the top of the footing at SW and NE yielded at 6.1-6.6 sec. Strains of these longitudinal bars except the inner longitudinal bars 150 mm below the top of the footing at SW exceeded over 10,000 μ . On the other hand, the maximum strains of longitudinal bars 300 mm or below the top of the footing is less than 2,000 μ . Therefore, longitudinal bars 300 mm or below from the top of the footing did not yield during C1-5(1)-1 excitation. During C1-5(1)-2 and C1-5(2) excitations, longitudinal bars 300 mm below the top of footing yielded while longitudinal bars 300 mm or below the top of footing did not yield.

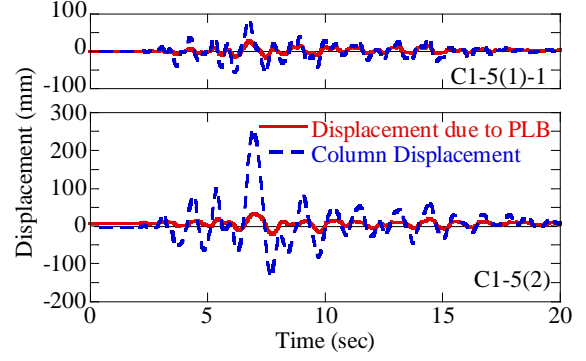


Figure 7. Column Displacement and Lateral Displacement at the Column Top due to PLB in the Principal Response Direction

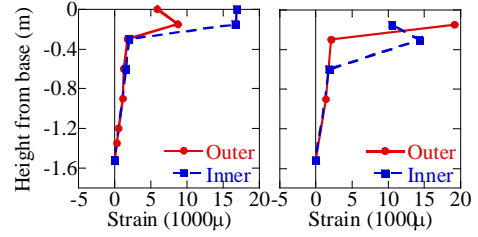


Figure 8. Strain of Longitudinal Bars in Footing when Column Displacement Reached its Peak

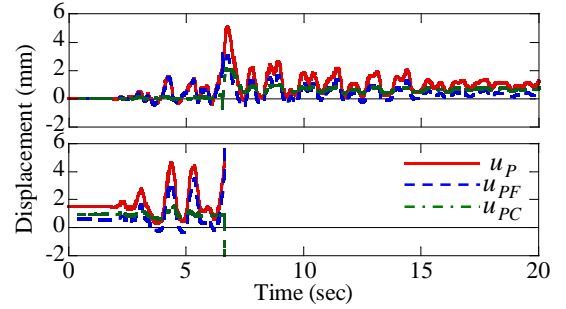


Figure 9. PLB Displacement of NE Longitudinal Bar

Fig. 9 shows PLB/F, PLB/C and PLB displacements, u_{PFi} , u_{PCi} and u_{Pi} , which are evaluated from the longitudinal bar strains and measured vertical displacement at the column base as

$$u_{PFi} = \int_{-H}^0 \varepsilon(z) dz = \sum_{j=1}^{N-1} \frac{1}{2} (\varepsilon_{j-1} + \varepsilon_j) (h_{j-1} - h_j) \quad (21)$$

$$u_{PCi} = u_1 - \frac{h_1}{h_2} u_2 - u_{PFi} \quad (22)$$

where ε_j is measured strain at point j , h_j is distance between point j and the top of the footing, N is number of measured strains, u_1 is measured vertical displacement between the top of the footing and 80 mm ($=h_1$) above the footing and u_2 is measured vertical displacement between 280 mm ($=h_2$) and 80 mm above the footing. The peak PLB and PLB/F displacements were 4-6 mm and 2-4 mm during C1-5(1)-1 and C1-5(2) excitations and did not increase even though response displacement increased because the moment acted at the column base did not increase.

Fig. 10 shows relations between column displacement and lateral displacement due to PLB in the principal response direction. The displacements computed using proposed model is also shown in Fig. 10 for comparison. Lateral displacement due to PLB, u_{Pp} , and lateral displacement ratio, r_p , is evaluated as,

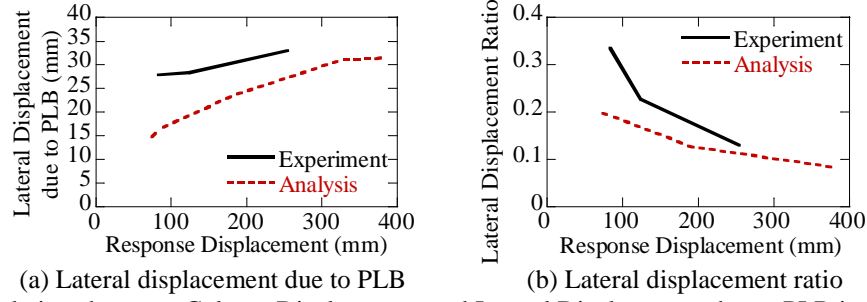


Figure 10. Relations between Column Displacement and Lateral Displacement due to PLB in the Principal Response Direction

$$\begin{aligned} u_{Px} &= \theta_y h_c \\ u_{Py} &= -\theta_x h_c \end{aligned} \quad (23)$$

$$\begin{aligned} u_{Pp} &= u_{Px} \cos \theta_p + u_{Py} \sin \theta_p \\ r_p &= \frac{\max |u_p(t)|}{\max |u(t)|} \end{aligned} \quad (24)$$

where h_c is column height, θ_p is angle to the principal response direction and θ_x and θ_y are column rotation to minimize summation of square of the error, $e = \sum_{i=1}^N \{u_{PFi} - (u_z + x_i \theta_x + y_i \theta_y)\}^2$.

The peak lateral displacement due to PLB did not increase even if the response displacement at the column top increased, while lateral displacement ratio decreased as the response displacement at the column top increased. This is because the peak moment at the column base did not increase as described above. Thus, lateral displacement ratio, r_p , is decreased as column displacement increases.

4. ANALYTICAL CORRELATION OF PROPOSED PLB MODEL

The column and experimental setup were idealized by a 3D discrete analytical model as shown in Fig. 11. The column was idealized by fiber elements. A section was divided into 400 fibers. The stress vs. strain constitutive model of confined concrete and unloading and reloading hysteresis of concrete were evaluated based on Hoshikuma et al. (1997) model and Sakai and Kawashima (2006) model. The stress vs. strain constitutive model of longitudinal bars was evaluated based on Menegotto-Pinto (1973) model modified by Sakai and Kawashima (2003). Proposed PLB interface element was set at the column base.

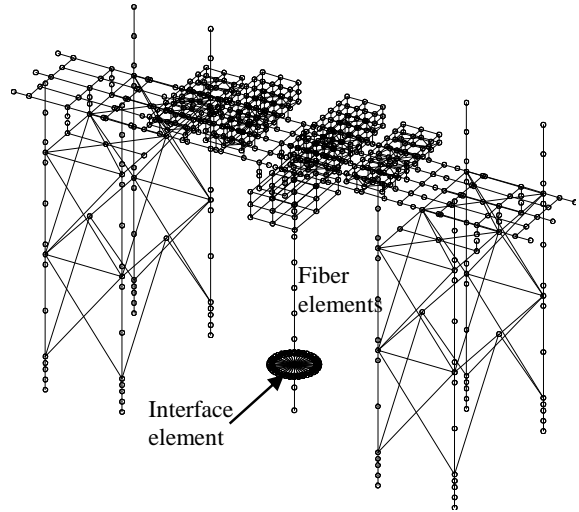


Figure 11. Analytical Model

The plastic strain development ratio β is assumed to be 1/4 because development length inside the footing defined as Eq. 8 is 1.12 m and the length of the region where the longitudinal bars yielded is about 0.3 m as shown in Fig. 8. The bond-degrading ratio γ is assumed to be 0.2 based on the result of C1-5 experiment.

Figs. 12 and 13 show response acceleration at the column top in the longitudinal direction and column displacement in the principal response direction during C1-5(1)-1 and C1-5(2) excitations. Response acceleration and displacement at the column top computed with and without PLB model correlate well

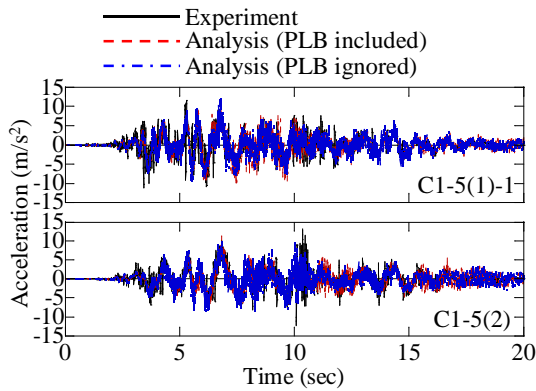


Figure 12. Response Acceleration at the Column Top in Longitudinal Direction

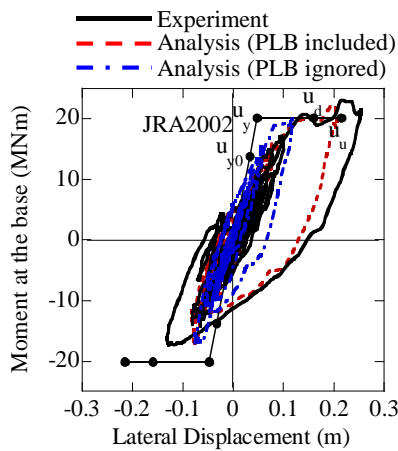


Figure 14. Moment at the Base vs. Column Displacement Hysteresis in the Principal Response Direction during C1-5(2) excitation

with experimental results during C1-5(1)-1 excitation. However, during C1-5(2) excitation, the peak displacement computed with proposed PLB model is 207 mm, which is 18 % smaller than measured displacement, while the peak displacement computed ignoring PLB is 119 mm, which is only 47 % of measured displacement. Proposed PLB model enhances the correlations of analytical results to experimental results.

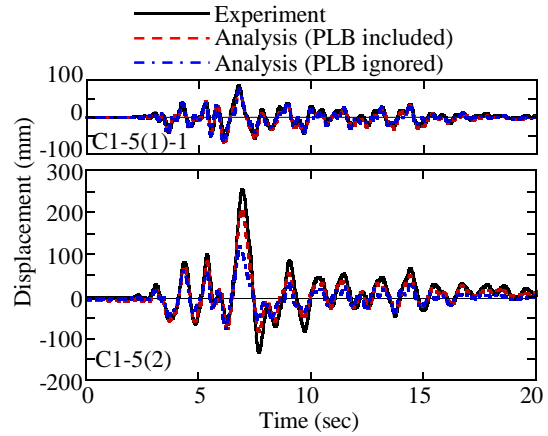


Figure 13. Computed Column Displacement in the Principal Response Direction

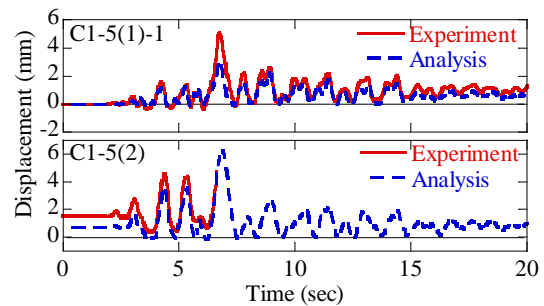


Figure 15. Computed PLB Displacement at NE Longitudinal Bar

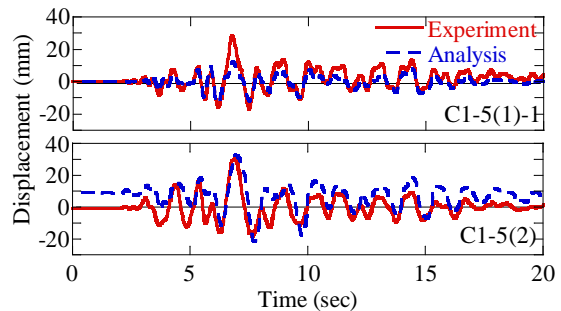


Figure 16. Computed Lateral Displacement at the Column Top due to PLB in the Principal Response Direction

Fig. 14 shows moment at the base vs. column displacement hysteresis in the principal direction during C1-5(2) excitation, Fig. 15 shows computed PLB displacement at NE longitudinal bars and Fig. 16 shows computed lateral displacement at the column top due to PLB in the principal response direction. Computed moment at the base, the computed pullout displacement due to PLB and the lateral displacement due to PLB also correlate well with experimental results.

As shown in Fig. 10, the computed lateral displacement due to PLB is 48-27 % smaller than measured displacement and computed lateral displacement due to PLB increases as response displacement increased until C1-5(3)-1 excitation and reaches maximum value of about 30 mm during C1-5(3)-1 and C1-5(3)-2 excitations.

5. CONCLUSIONS

An analytical model for taking account of pulling out of longitudinal bars in the footing and the column (PLB) was developed and verified based on full-scale RC bridge column used in E-Defense shake table experiment. Based on the analytical studies presented herein, the following conclusions may be deduced;

1) The strain of the longitudinal bars in the footing occurred between the top of the footing and 1350 mm below the top of the footing. The longitudinal bars yielded between the top of the footing and 300 mm below the top of the footing yielded.

2) The maximum lateral displacement at the column top due to PLB was 28 mm, 28 mm and 33 mm during C1-5(1)-1, C1-5(1)-2 and C1-5(2) excitations, respectively. The maximum lateral displacement at the column top due to PLB did not increase even though the response displacement at the column top increased because the moment acted at the column base reached the moment capacity of the column and did not increase. Therefore, the lateral displacement ratio defined as the ratio of the maximum lateral displacement at the column top due to PLB to the maximum total response displacement at the column top was 0.33, 0.22 and 0.13 during C1-5(1)-1, C1-5(1)-2 and C1-5(2) excitations, respectively, and it decreased as response displacement increased.

3) Response displacement at the column top as well as the pullout displacement due to PLB, which were computed by fiber element analysis with the developed PLB interface element model, correlates well with results of C1-5 experiment. Implementation of the PLB model enhances the analytical correlation to the C1-5 experiment.

AKNOWLEDGEMENT

The C1-5 experiment was conducted based on the extensive support of over 70 personnel in the Overview Committee (Chair, Professor Emeritus Hirokazu Iemura, Kyoto University) and Executing Committee of Large-scale Bridge Experimental Program (Chair, Professor Kazuhiko Kawashima, Tokyo Institute of Technology) Their strong support is greatly appreciated. The appreciation is extended to Mr. Hiromichi Ukon and Professor Manabu Nakayama for his enthusiastic contribution to the project.

REFERENCES

- Imai, K., Korenaga, T. and Takiguchi, K. (2005). A Method for Analyzing Rotation at the Base of Reinforced Concrete Member considering Sinking and Pullout, *Journal of Structural and Construction Engineering*, Transactions of AIJ, **Vol. 589**, pp. 149-156.
- Kawashima, K., Sasaki, T., Kajiwara, K., Ukon, H., Unjoh, S., Sakai, J., Kosa, K., Takahashi, Y., Yabe, M. and Matsuzaki, H. (2009). Shake table experiment on RC bridge columns using E-Defense, *Proc. 41st Panel on Wind and Seismic Effects*, UJNR, Public Works Research Institute, Tsukuba Science City, Japan.
- Morita, S. (1969). Bond and Cracks in Reinforced Concrete, *Concrete Journal*, JCI.
- Menegotto, M. and Pinto, P. E. (1973). Method of analysis for cyclically loaded R.C. plane frames force and bending, *Proc. IABSE Symposium on Resistance and Ultimate Deformability of Structures Acted on by Well Defined Repeated Loads*, pp. 15-22.
- Popov, E. P. (1984). Bond and anchorage of reinforcing bars under cyclic loading, *ACI Journal*, **No. 81-31**, pp. 340-349.
- Priestley, N.M.J., Seible, F. and Calvi, M. (1996). *Seismic design and retrofit of bridges*, John Wiley & Sons, New York, USA.
- Sakai, J. and Kawashima, K. (2003). Modification of the Giuffre, Menegotto and Pinto model for unloading and reloading paths with small strain variations, *Journal of Structural Mechanics and Earthquake Engineering*, JSCE, **738/I-64**, pp. 159-169.
- Shima, H., Chou, L. L. and Okamura, H. (1987). Bond Characteristics in Post-Yield Range of Deformed Bars, *Journal of Structural Mechanics and Earthquake Engineering*, JSCE, **378/V-6**, pp. 213-220.